The Astrophysical Journal, 732:113 (8pp), 2011 May 10 doi:10.1088/0004-637X/732/2/113

BROAD Lyα EMISSION FROM THREE NEARBY BL LACERTAE OBJECTS

John T. Stocke[1], Charles W. Danforth[1], and Eric S. Perlman[2]
[1] CASA, Department of Astrophysical and Planetary Sciences, University of Colorado, 389-UCB, Boulder, CO 80309, USA; danforth@casa.colorado.edu, stocke@casa.colorado.edu
[2] Florida Institute of Technology, Physics and Space Sciences Department, 150 West University Boulevard, Melbourne, FL 32901, USA; eperlman@fit.edu
Received 2010 October 25; accepted 2011 March 10; published 2011 April 25

ABSTRACT

We present far-UV *HST*/COS spectra of four nearby BL Lac objects. BL Lac spectra are dominated by a smooth, power-law continuum which arises in a relativistic jet. However, the spectra are not necessarily featureless; weak, broad- and/or narrow-line emission is sometimes seen in high-quality optical spectra. We present detections of Lyα emission in *HST*/COS spectra of Mrk 421 ($z = 0.030$) and PKS 2005−489 ($z = 0.071$) as well as an archival *HST*/GHRS observation of Mrk 501 ($z = 0.0337$). Archival *HST*/STIS observations of PKS 2155−304 ($z = 0.116$) show no Lyα emission to a very low upper limit. Using the assumption that the broad-line region (BLR) clouds are symmetrically placed around the active galactic nucleus (AGN), we use these measured Lyα emission features to constrain either the relativistic Γ values for the ionizing continuum produced by the jet (in the ionization-bounded case) or the mass of warm gas (in the density-bounded case). While realistic Γ values can be obtained for all four cases, the values for Mrk 421 and PKS 2155−304 are high enough to suggest that covering factors of BLR clouds of ∼1%–2% might be required to provide consistency with earlier values of Doppler boosting and viewing angles suggested for this class of BL Lacs. This discrepancy also exists in the case of M 87, where the amount of Doppler boosting in our direction is expected to be minimal, again suggestive of a small covering factor of BLR clouds. If, as these small covering factors might suggest, the assumptions of a density-bounded model could be more correct, then the observed Lyα luminosities require that BL Lac/FR 1 nuclei possess very little warm gas (10^{-4} to 10^{-5} $M_{\odot}$) as suggested by Guilbert et al. If these clouds are in pressure balance with a hotter (∼10^6 K) gas, the BLR contains too little mass to power the AGN by accretion alone.

Key words: BL Lacertae objects: general – BL Lacertae objects: individual (Mrk 421, PKS 2005−489, Mrk 501, PKS 2155−304) – galaxies: nuclei – quasars: emission lines – ultraviolet: galaxies

Online-only material: color figures

1. INTRODUCTION

BL Lacertae objects (BL Lacs hereafter) are an extreme type of active galactic nuclei (AGNs) in which the non-thermal continuum emission is thought to be relativistically beamed and Doppler-boosted, overwhelming thermal sources of emission seen in most other AGN classes. These sources, together with the flat-spectrum radio quasars, are the most numerous and most luminous AGNs at photon energies greater than a few hundred keV (e.g., Abdo et al. 2009). While there are a few BL Lacs that completely lack optical emission lines (e.g., Rector & Stocke 2001; Sbarufatti et al. 2006), high signal-to-noise ratio (S/N) optical spectroscopy often detects weak but moderately luminous emission lines, especially in objects with spectral energy distributions (SEDs) that peak in the infrared ("low-frequency peaked BL Lacs" or LBLs; e.g., Stickel et al. 1993; Scarpa & Falomo 1997; Rector & Stocke 2001; Corbett et al. 2000) like BL Lac itself (Vermeulen et al. 1995).

Less is known about the emission line regions of the high-energy peaked BL Lacs (HBLs; Padovani & Giommi 1995), which have SEDs peaking in the UV to X-rays and extended radio emission consistent with being Fanaroff & Riley (1974) type 1 (FR 1s) (Perlman & Stocke 1993; Rector & Stocke 2001; Giroletti et al. 2008). Most HBLs have no detectable optical line emission (Rector & Stocke 2001; Sbarufatti et al. 2006). It is possible that emission lines comparable to FR 1s (weak Hα+[N II] and/or weak [O II]; e.g., in Mrk 501; Antonucci 1984) are present in many HBLs but are hidden at optical wavelengths by the non-thermal AGN continuum and by starlight from the host galaxy (Browne & Marchã 1993). On the other hand, many HBLs possess optical spectra which contain the absorption lines and edges (e.g., Ca II H&K break, *G* band) typical of giant elliptical galaxies that are the usual hosts of these AGN (Hutchings & Neff 1992; Wurtz et al. 1996; Scarpa et al. 2000; Sbarufatti et al. 2005).

While the LBL/HBL distinction may be a result of previous selection techniques (as suggested by Collinge et al. 2005), the observed properties of these two classes do vary; all HBLs and most LBLs have radio emission consistent with being beamed FR 1s (Rector et al. 2000), while some LBLs are consistent with beamed emission from the more powerful Fanaroff–Riley class 2 (FR 2s) sources like the flat-spectrum radio quasars (e.g., Brinkmann et al. 1996; Rector & Stocke 2001). Setting aside the few FR 2-like LBLs, most BL Lacs can be explained as beamed FR 1 radio galaxies. It is unclear whether the differences between LBLs and HBLs are a consequence of viewing angle (Perlman & Stocke 1993; Jannuzi et al. 1994; Rector & Stocke 2001; Nieppola et al. 2008), peak frequencies and luminosities (the so-called Blazar sequence; see Fossati et al. 1998; Ghisellini et al. 1998, 2002; Cavaliere & D'Elia 2002; Guetta et al. 2004; Maraschi et al. 2008; Ghisellini & Tavecchio 2008), or a combination of both geometric and intrinsic factors (Georganopoulos & Marscher 1998).

Broad-line emission is an essential property of AGNs and can provide insights on a number of properties. Fundamentally, the line luminosities represent a direct measure of the amount of circumnuclear gas at parsec scales and the isotropic, ionizing photon environment. Direct measurement of the luminosity of

Table 1
Observation Summary

BL Lac Object	R.A. (J2000) Decl.	z_{AGN}	Instrument	t_{exp}	Obs. Date
Mrk 421	11:04:27+38:12:32	0.0300	COS/G130M	1738	2009 Dec 24
			COS/G160M	2404	2009 Dec 24
PKS 2005−489	20:09:25−48:49:54	0.0710	COS/G130M	2462	2009 Sep 21
			COS/G160M	1854	2009 Sep 21
Mrk 501	16:53:52+39:45:37	0.0337	GHRS/G160M	29196	1992 Feb 26–28
PKS 2155−304	21:58:52−30:13:32	0.116	STIS/E140M	14244	1999 Nov 9
				14244	2000 Sep 26

the broad-line region (BLR) in BL Lacs can provide a new, direct measurement of the radiative power of these AGNs and so can provide an independent constraint on the amount of beaming. Current evidence suggests that the luminosity of any broad emission lines in BL Lacs may be linked to the synchrotron peak frequency as originally suggested by Georganopoulos & Marscher (1998) and Ghisellini et al. (1998). If BLR photons are abundant, the cooling of the jet's synchrotron emission is enhanced greatly by the increased inverse-Comptonization of these photons by the jet. This increased cooling will decrease the peak frequency of the jet emission, resulting in a peak at IR energies or below (i.e., LBLs). However, without BLR seed photons, the jet cooling will be dominated by the synchrotron process and so is much less efficient. This results in a much higher frequency synchrotron peak, in the UV or X-rays (i.e., HBLs).

Is the lack of observed line emission in BL Lacs, particularly HBLs, an intrinsic property of these less luminous AGNs, or is it a product of the photon environment induced by the jet? The creation of stable BLR clouds may be inhibited by soft X-ray spectra (Guilbert et al. 1983) which are observed in only one of the two BL Lac classes. In the case of LBLs, the X-ray emission is relatively weak and the X-ray spectrum is hard ($\alpha_x < 1$; Urry et al. 1996; Padovani et al. 2004). In HBLs the X-rays are quite luminous ($L_X = 10^{44}$–10^{46} erg s^{-1}) and soft (power-law spectral index in energy $= -1$ to -2.8; Perlman et al. 1996, 2005; Padovani et al. 2001). Thus, the soft X-ray continuum seen in HBL-type objects may be impeding their ability to create BLR clouds. This can be confirmed by observational data using Lyα, the most sensitive probe of BLR gas.

In this paper, we present far-ultraviolet (FUV) spectroscopy of four of the nearest HBL prototypes, in which weak Lyα emission lines have been detected or sensitive upper limits can be set. In Section 2, we present new high S/N spectra from the Cosmic Origins Spectrograph (COS), newly installed on the *Hubble Space Telescope* (*HST*), of Mrk 421 and PKS 2005−489, an archival Goddard High Resolution Spectrograph (GHRS) spectrum of Mrk 501, and an archival Space Telescope Imaging Spectrograph (STIS) spectrum of PKS 2155−304. We measure Lyα line widths and luminosities and reddening-corrected continuum luminosities and slopes for these HBLs.

These observations provide the first simultaneous measurements of continuum and BLR line emission in HBLs. In Section 3, we use the observed continua to derive ionizing luminosities and thereby predict the Lyα line luminosities under the "nebular hypothesis" (ionization-bounded case). Comparison between the predicted and observed Lyα luminosity allows an estimate of the beaming angle for the ionizing flux. Using the density-bounded assumption allows us to compute the amount of warm BLR gas assuming that the gas is optically thin.

2. BL LAC OBSERVATIONS AND ANALYSIS

We present new COS FUV spectra of two BL Lac targets (Mrk 421 and PKS 2005−489) as well as archival observations of Mrk 501 (GHRS) and PKS 2155−304 (STIS). The four targets are summarized in Table 1.

COS FUV observations of Mrk 421 and PKS 2005−489 were carried out during the first three months of COS science observations as part of the COS Guaranteed Time Observations (PID 11520, PI: Green). Four exposures were made in each of the G130M (1135 Å $< \lambda <$ 1480 Å) and G160M (1400 Å $< \lambda <$ 1795 Å) medium-resolution gratings ($R \approx 18,000$) for each target. Four central wavelength settings at each grating dithered known instrumental features along the spectrum and provided continuous spectral coverage over 1135 Å $< \lambda <$ 1795 Å (see J. Green et al. 2011, in preparation; Osterman et al. 2010).

All COS exposures were reduced using CalCOS v2.11f. Flat fielding, alignment, and co-addition of the processed exposures were carried out using IDL routines developed by the COS GTO team specifically for COS FUV data.[3] The details of the co-addition method are discussed in Danforth et al. (2010). Briefly, each exposure was corrected for narrow, ∼15% opaque shadows from repeller grid wires. The local exposure time in these regions was reduced to give them less weight in the exposure-weighted final co-addition. Similarly, exposure times for data at the edges of the detectors were de-weighted. With four different central wavelength settings per grating, any residual instrumental artifacts from grid-wire shadows and detector boundaries have negligible effect on the final spectrum.

Strong ISM absorption features in each exposure were aligned via cross-correlation and interpolated onto a common wavelength scale. The wavelength shifts were typically of the order of a resolution element (∼0.07 Å, ∼17 km s^{-1}) or less. The co-added flux at each wavelength was taken to be the exposure-weighted mean of flux in each exposure. To quantify the quality of the combined data, we identify line-free continuum regions at various wavelengths, smooth the data by the 7 pixel resolution element, and define S/N (≡ mean(flux)/stddev(flux)) ≈ 37 and ≈20 for the Mrk 421 and PKS 2005−489 observations, respectively. The fully reduced, co-added spectra of Mrk 421 and PKS 2005−489 are shown in Figure 1.

In addition to the two COS data sets, we analyze archival observations of the BL Lac objects Mrk 501 (GHRS) and PKS 2155−304 (STIS). Mrk 501 was observed for 29 ks with the G160M grating covering 1222 Å $< \lambda <$ 1257 Å at an FWHM of ∼20 km s^{-1} and S/N ≈ 15. PKS 2155−304 was observed for 28.5 ks with the STIS/E140M grating (1140 Å $< \lambda <$ 1729 Å), FWHM ∼ 7 km s^{-1}, S/N ≈ 27. Details of the GHRS

[3] See http://casa.colorado.edu/∼danforth/costools.html for our co-addition and flat-fielding algorithm and additional discussion.

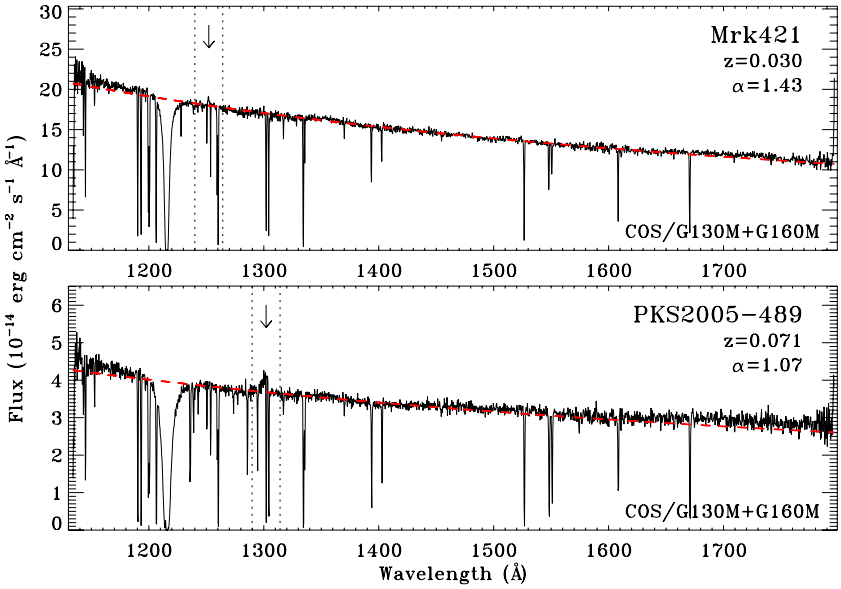

Figure 1. COS observations of Mrk 421 (top) and PKS 2005−489 (bottom) over the entire COS/G130M+G160M range. The flux has been corrected for reddening and is shown binned by 30 pixels (∼4 resolution elements). Power-law continua of the form $F(\lambda) = I_0 * (\lambda/912)^{-\alpha_\lambda}$ were fitted to line-free continuum regions and are shown as dashed curves. The narrow absorption features are mostly interstellar absorption lines; a few lines blueward of Lyα are intergalactic. The region around the rest-frame Lyα (arrow) bounded by vertical dotted lines is expanded in Figure 2 below.

(A color version of this figure is available in the online journal.)

and STIS data sets and reduction techniques can be found in Penton et al. (2000) and Indebetouw & Shull (2004), respectively.

In order to accurately measure BL Lac continua, the observations were corrected for Galactic extinction. Traditional measures of extinction are based on broad-beam radio observations of Galactic H I emission and may not take into account small-scale variations in this value. Since three out of four of our data sets cover the region around Galactic Lyα absorption, we can directly measure $N_{\rm H\,I}$ and calculate the extinction, $E(B-V)$, along our sight line via the relationship $E(B-V) = N_{\rm H\,I}/5.8 \times 10^{21}\,{\rm cm}^{-2}$ (Shull & van Steenberg 1985). Uncertainties in fitted Galactic $N_{\rm H\,I}$ and the resulting errors in extinction correction dominate the subsequent uncertainties in continuum fitting. In Figure 1, the best-fit reddened power laws show some systematic deviation at both the long- and short-wavelength ends for unknown reasons—a single power-law index may not be applicable, the COS flux calibration may not be correct, or the FUV extinction correction may be deficient. These discrepancies do not affect our measurements of Lyα emission although the continuum flux at $\lambda < 912$ Å may be underestimated by ∼10%. The Mrk 501 observations do not include 1216 Å, so we use the literature extinction value for this sight line. Observed spectra were corrected for Galactic reddening via the Fitzpatrick (1999) parameterization.

Dereddened spectra were next blueshifted into the rest frame of the BL Lac and line-free continuum regions were identified and fitted with a power law of the form $F_\lambda = I_0\,(\lambda/912)^{-\alpha_\lambda}$. The region near rest-frame Lyα was not included in the fits. Flux at the rest-frame Lyman continuum is derived via a short extrapolation from the *HST* spectra. The Mrk 501 GHRS data have such a small wavelength coverage that the continuum fit slope and LyC extrapolation are uncertain.

Next, the Lyα emission feature was measured (Figure 2). All three observed emission features were well fitted with single Gaussian profiles with free parameters $v_{\rm centroid}$, FWHM, and integrated intensity I(Lyα). Total Lyα luminosity (assuming isotropy) is then $L({\rm Ly}\alpha) = I({\rm Ly}\alpha)\,4\pi(c\,z_{\rm em}/H_0)q^2$ with $H_0 = 72\,{\rm km\,s^{-1}\,Mpc^{-1}}$. The significance of these features can be estimated as

$$\mathrm{SL} \approx \sqrt{C}\,\frac{W(\mathrm{S/N_{res}})}{\sqrt{\mathrm{FWHM}}}, \qquad (1)$$

where the scaling constant C is equal to the number of resolution elements per Å, W is the equivalent width of the line, $\mathrm{S/N_{res}}$ is the signal-to-noise per resolution element, and FWHM is the full width at half-maximum of the emission line. This comes to $\sim 9\sigma$, $\sim 15\sigma$, and $\sim 23\sigma$ for Mrk 421, PKS 2005−489, and Mrk 501, respectively.

No Lyα emission is seen in the spectrum of PKS 2155−304 (Figure 2). If we assume FWHM ∼ 3 Å for the emission line width we find a 4σ upper limit of $W \lesssim 44$ mÅ or $I({\rm Ly}\alpha) \lesssim 4 \times 10^{-15}\,{\rm erg\,cm^{-2}\,s^{-1}}$. Given the higher continuum luminosity of PKS 2155 + 304, the Lyα luminosity upper limit ($L({\rm Ly}\alpha) \lesssim 1.1 \times 10^{41}\,{\rm erg\,s^{-1}}$) is comparable to the detections in the other HBLs.

All of the measured and derived quantities discussed above are listed in Table 2 for each of the four BL Lacs.

Neither Mrk 421 nor PKS 2005−489 show emission from the C IV λλ1548, 1550 doublet. Due to the lower effective area of COS at the red end of the FUV range, these data are of lower S/N than those covering the Lyα emission region. We derive upper limits on C IV emission for these two objects of $I_{\rm C\,IV} \lesssim 0.8 \times 10^{-14}\,{\rm erg\,cm^{-2}\,s^{-1}}$ and $I_{\rm C\,IV} \lesssim 4.3 \times 10^{-14}\,{\rm erg\,cm^{-2}\,s^{-1}}$ for Mrk 421 and PKS 2005−489, respectively. The spectra of the other two BL Lac objects do not cover the rest-frame $\lambda \sim 1549$ Å region.

3. INFERENCES FOR THE BROAD-LINE REGIONS OF BL Lacs

With both continuum and emission-line measurements, we can estimate the covering fraction and beaming angle for BL Lacs under the nebular hypothesis. To start we assume that the covering factor of the BLR clouds is 100% and the

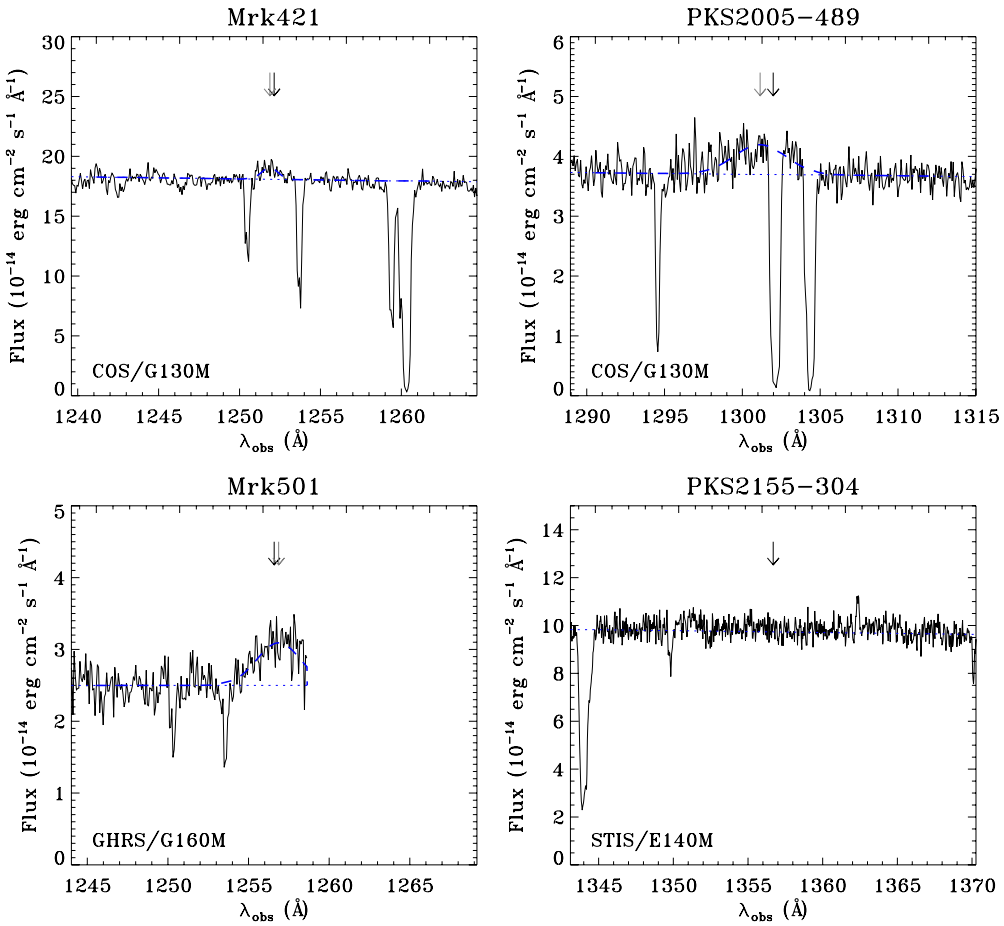

Figure 2. Detailed spectra of the Lyα region in each BL Lac. All data are dereddened, binned to ~15–20 km s^{-1}, and shown over the range $cz_{\rm AGN}$ = $\pm$3000 km s^{-1}. Power-law continuum fits are shown as dotted lines. Black arrows mark the systemic velocity of Lyα using the absorption-line redshifts for these objects. Thick dashed curves show Gaussian Lyα fits for the three detections and line centroid locations are marked with gray arrows. Full fit parameters are given in Table 2. All narrow absorption features are intervening interstellar or intergalactic absorption features unrelated to the AGN emission. The Lyα emission feature from Mrk 501 falls at the edge of the GHRS data.

(A color version of this figure is available in the online journal.)

clouds are spherically distributed around the nucleus. From this simple geometry other geometries can be assumed, so that these calculations can be used as baseline values. First, we estimate the total ionizing flux in the BLR by extrapolating the power-law continuum to higher energies. Next, we predict the resulting BLR Lyα line emission assuming that (1) the ionizing flux is isotropic (clearly a poor assumption for BL Lacs) and (2) the broad-line clouds are optically thick to ionizing photons with unity covering factor (i.e., the "nebular hypothesis" or ionization-bounded case) or (3) the BLR clouds are optically thin individually and in toto (the density-bounded case). We will then interpret the difference between the predicted and observed Lyα luminosities in the ionization-bounded case to determine if the required Doppler boosting is consistent with estimates from other considerations. And then we use the Lyα line luminosities to infer BLR warm gas mass in the density-bounded case.

3.1. Ionization-bounded Model

Under Case-B recombination, the number of photons emitted in a given line (e.g., Hβ) can be related to the total number of ionizing photons by the ratio of their recombination coefficients (see Equation (5.40) of Osterbrock & Ferland 2006),

$$\frac{L(\mathrm{H}\beta)}{h\,\nu_{\mathrm{H}\beta}} \approx \left(\frac{\alpha^{\rm eff}_{\mathrm{H}\beta}}{\alpha_B}\right) \int_{\nu_0}^{\infty} \frac{L(\nu)}{h\,\nu}\,d\nu, \qquad (2)$$

where the effective $\alpha^{\rm eff}_{\mathrm{H}\beta} = 3.03 \times 10^{-14}\,\mathrm{cm^{-3}\,s^{-1}}$ and $\alpha_B = 2.59 \times 10^{-13}\,\mathrm{cm^{-3}\,s^{-1}}$ for Case-B recombination at $T \sim 10^4$ K. Lyα luminosity L(Lyα) is then related to L(Hβ) by the ratio of their respective specific intensities,

$$\frac{j_{\mathrm{Ly}\alpha}}{j_{\mathrm{H}\beta}} = \left(\frac{h\nu_{\mathrm{Ly}\alpha}}{h\nu_{\mathrm{H}\beta}}\right)\left(\frac{\alpha_B}{\alpha^{\rm eff}_{\mathrm{H}\beta}}\right) \approx 34 \qquad (3)$$

under Case-B recombination. Substituting the power law fitted to the observed BL Lac spectra, Equation (2) becomes

$$I(\mathrm{H}\beta)_{\rm predicted} = h\nu_{\mathrm{H}\beta}\left(\frac{\alpha^{\rm eff}_{\mathrm{H}\beta}}{\alpha_B}\right)\frac{I_0\,\lambda_0^2}{c}\int_{\nu_0}^{\infty}\frac{1}{h\nu}\left(\frac{\nu}{\nu_0}\right)^{-(2-\alpha_\lambda)} d\nu \qquad (4)$$

and the predicted Lyα flux is

$$I(Ly\alpha)_{\rm predicted} = 4\left(\frac{\alpha_B}{\alpha^{\rm eff}_{\mathrm{H}\beta}}\right) I(\mathrm{H}\beta)_{\rm predicted}. \qquad (5)$$

The Lyα emission predicted from the power-law continuum fit overpredicts the observed Lyα emission by 2–4 orders of magnitude in all four cases (Table 2). The simplest interpretation of the Lyα overprediction is that the ionizing continuum seen by the BLR clouds is 2–4 orders of magnitude less intense than what we see (i.e., beaming). In this case, we can use the

Table 2
BL Lac Measured and Derived Quantities

Quantity	Mrk 421	PKS 2005−489	Mrk 501	PKS 2155−304	Units
z_{em}	0.030	0.071	0.03366	0.116	
log N(H I)	20.04 ± 0.03	20.49 ± 0.03	20.04:[a]	19.96 ± 0.03	
$E(B-V)$	0.019 ± 0.002	0.053 ± 0.004	0.019:[a]	0.016 ± 0.001	
S/N$_{res}$	37	20	15	27	(see the text)
Continuum fit: $F_\lambda = I_0\,(\lambda/912)^{-\alpha_\lambda}$					
α_λ	1.43 ± 0.02	1.07 ± 0.04	0.7 :	1.13 ± 0.01	
I_0	27.2 ± 0.6	5.01 ± 0.22	3.0 :	13.4 ± 0.2	(10^{-14} erg cm^{-2} s^{-1} Å^{-1})
X-ray spectral fit parameters[b]					
a	2.10–2.58	2.36–3.14	1.41–2.18	2.3–2.8	
b	0.31–0.46	0.27 ± 0.09	0.12–0.56	−0.3–0.65	
Lyα emission feature					
$\lambda_{centroid}$	1251.9	1301.1	1256.9	1357[c]	(Å, observed)
$v_{Ly\alpha} - v_{em}$	−60	−190	+70	···	(km s^{-1})
FWHM	1.23 ± 0.13	4.25 ± 0.24	3.31 ± 0.33	3[c]	(Å)
FWHM	300 ± 30	1050 ± 60	820 ± 80	740[c]	(km s^{-1})
Equivalent width	−76 ± 7	−467 ± 47	−830 ± 83	<44	(m Å)
Significance level	9	15	23	<4	(σ)
I(Lyα)	1.27 ± 0.12	2.38 ± 0.11	2.2 ± 0.2	$\lesssim$0.4	(10^{-14} erg cm^{-2} s^{-1})
L(Lyα)	2.37 ± 0.22	24.9 ± 1.1	5.2 ± 0.3	$\lesssim$11	(10^{40} erg s^{-1})
Predicted Lyα Emission					
I(Lyα)$_{predicted}$	3.0×10^{-10}	3.6×10^{-11}	$\sim 10^{-11}$	1.0×10^{-10}	(erg cm^{-2} s^{-1})
Overprediction factor (OPF)	2.4×10^4	1.5×10^3	∼600	$>2.6 \times 10^4$	
Doppler factor (δ)[d]	16.6	6.5	∼4	>13.6	
Minimum required (Γ)[d]	8.3	3.2	∼2	>6.8	
Maximum viewing angle[d]	3.5	8.8	∼16	<4	(°)

Notes.
[a] Literature value; not directly measured.
[b] X-ray spectral fit parameters as defined in Perlman et al. (2005): $dN/dE \propto E^{[-a+b\,\log(E)]}$. Parameter ranges are taken from the literature of the last 10 years (Acciari et al. 2009; Brinkmann et al. 2001, 2003, 2005; Donato et al. 2005; Edelson et al. 2001; Foschini et al. 2006; Massaro et al. 2008; Padovani et al. 2001; Ravasio et al. 2004; Sembay et al. 2002; Tramacere et al. 2007a, 2007b; Zhang et al. 2006a, 2006b; Zhang 2008).
[c] Assumed quantity; see the text.
[d] Assuming unity covering factor of BLR clouds.

overprediction factor (OPF) to calculate a required beaming factor ($\delta = [\Gamma(1 - \beta\,\cos\,\theta)]^{-1}$, where the relativistic Γ and β are as usually defined and θ is the "viewing angle" between the outflow axis and the observer's line of sight), the minimum required Γ of the outflow and the maximum allowed viewing angle all assuming a unity covering factor of BLR clouds as seen from the source. Since the bulk of the ionization of the BLR clouds is due to photons just blueward of the Lyman limit, the OPF $= \delta^{3+\alpha_\nu}$, where the power-law spectral index in frequency $\alpha_\nu = (\alpha_\lambda + 2)$ (see Table 2). See Appendices A and B of Urry & Padovani (1995) for equations and derivations. The exponent on δ is appropriate for a spherical cloud morphology of the emitting region; a continuous, cylindrical morphology yields one less power on this exponent and thus more extreme values of Γ than we quote in Table 2. Also, these expressions may not be exact in these BL Lacs because we do not directly observe the flux and spectrum of the ionizing radiation as a function of all off-axis angles; we are assuming that the dominant off-axis ionizing radiation source is the relativistic jet.

On the other hand, for the large majority of viewing angles, the dominant UV/X-ray photon source may be the nuclear region of the AGN, not the jet. BL Lacs and their likely parent population of FR 1 galaxies have little or no disk emission suggesting a very low accretion rate in a radiatively inefficient accretion flow (Allen et al. 2006) onto their central black holes. As discussed in Allen et al. (2006), such a flow will also have a soft X-ray spectrum, albeit one that is thermal in shape, with a typical temperature of 0.5–1 keV. If the Lyα BLR emission we observe in these BL Lacs is due to thermal accretion emission then the value for the OPF only sets lower limits on Γ and δ since the off-axis jet emission must be even less luminous than what we have assumed for the values in Table 2. Either this thermal spectrum or the off-axis jet spectrum (which peaks in the FUV—soft X-ray with a soft X-ray spectrum, as described in, e.g., Perlman et al. 2005) would be hostile to the formation of BLR clouds (see below).

While the values of δ, minimum Γ, and maximum viewing angle in Table 2 are reasonable in the context of some HBLs (Hovatta et al. 2009; Ghisellini et al. 2010), Γ = 3–5 and $\theta = 10°$ are suggested from other considerations (Urry & Padovani 1995; Giroletti et al. 2006); $\Gamma = 3$ is suggested from luminosity function comparisons of HBLs and FR 1 radio galaxies (Urry & Padovani 1995) and Γ = 3–5 is suggested from radio core-to-extended flux ratios (Perlman & Stocke 1993; Rector et al. 2000; Giroletti et al. 2006). Therefore, the Γ values in Table 2 for Mrk 421 and PKS 2155−304 are somewhat too high to be consistent with earlier estimates. If we use the best previous values for Γ and θ quoted above to determine δ, we can then use the observed OPF to obtain a best estimate of the BLR cloud covering factor. In this case, values of 1%–2% are found. Such low covering factors are much more consistent with the expectation of the density-bounded model. However, it is equally

possible that the values of Γ in the Mrk 421 and PKS 2155-304 jets are significantly higher than estimates from entire samples of HBLs and so are consistent with an ionization-bounded model. Indeed, by assuming that the ionization-bounded model is correct, the values of Γ in Table 2 are the first such estimates using this method.

As a conceptual check of our methodology, we perform the equivalent analysis on a representative unbeamed AGN with strong Lyα emission. Seyfert galaxies lack the relativistic jets of radio-loud AGNs and the anisotropy of their emission is presumed to be low. Recent *HST*/COS observations of the nearby Sy 1.5 galaxy Mrk 817 show strong Lyα emission (I(Lyα) = 8.1×10^{-12} erg cm^{-2} s^{-1}) and a power-law continuum with parameters $I_0 = 1.5 \times 10^{-13}$ erg cm^{-2} s^{-1} and $\alpha_\lambda = 1.3$ (Winter et al. 2011). We extrapolate the AGN continuum via the Haardt & Madau (1996) spectrum for Akn 120 (another nearby Seyfert galaxy) and calculate the total ionizing flux as above. The predicted Lyα line emission is 2.7×10^{-11} erg cm^{-2} s^{-1}, a factor of only ∼3 higher than observed. Given that a Lyman limit break is not observed in this class of objects, a covering factor of $f_{\rm BLR} \sim 30\%$ is reasonable.

A second more relevant comparison for our inferences is the case of M87, the FR 1 radio galaxy Virgo A. Sankrit et al. (1999) presented an *HST*/Faint Object Spectrograph (FOS) spectrum of the nucleus of M87 arguing that the detected Lyα emission had to be primarily nuclear, photoionized emission by comparison to a second spectrum taken through an aperture displaced 0.6 arcsec nearby. The Lyα emission of M87 is at low enough redshift that it is significantly affected by Galactic Lyα absorption, whose influence can only be estimated very roughly. Sankrit et al. (1999) estimate that M87's intrinsic Lyα is at least a factor of two larger than the 9×10^{-14} erg cm^{-2} that they measure. If we use double their value for the Lyα flux and take the observed continuum flux extrapolated to 912 Å using a ν^{-1} power law typical of the four BL Lacs presented here, a value of OPF = 100–200 is obtained. The Sankrit et al. (1999) observations are consistent with this spectral index but have a wavelength range too small to determine an accurate α_ν. This large OPF is intriguing given the observed spectral properties of M87 and its inferred substantial off-axis viewing angle (25°; Heinz & Begelman 1997). The minimum values of Γ required by the large jet-to-counterjet ratio for the M87 jet (3–5) suggest that the continuum is not substantially beamed in our direction ($\delta \sim$ 1.5–2 or less if Γ is larger) so that the OPF should be quite low, 5–10 times lower than what we find. While other modeling of apparent superluminal motions within the jet (Biretta et al. 1999) suggests slightly smaller viewing angles (∼19°), somewhat larger values for Γ are required by these motions, again suggesting minimal beaming in our direction. Additionally, some of the nuclear Lyα emission could be shock-heated (Dopita et al. 1997) which would further reduce the amount attributable to the ionizing continuum. As with our more extreme BL Lac objects the high OPF for M87 suggests a low covering factor of a few percent for the BLR clouds. Since in the case of M87 there is less chance for misinterpretation due to potentially large beaming factors, these low covering factors are again suggestive of the density-bounded case.

3.2. Density-bounded Model

A second physical interpretation is that the Lyα overprediction is not due to beaming but due to the physical conditions in the distribution of the BLR clouds; i.e., the clouds themselves are optically thin and may also have small covering factor so that most of the ionizing photons simply escape regardless of the beaming. The 1%–2% covering factors found by applying best values to the ionization-bounded case may be indicative that the density-bounded case is more correct for this class of objects (HBLs and FR 1 radio galaxies). Up to now we have assumed a large-scale isotropic distribution of optically thick clouds; however, they may be optically thin and/or anisotropic. The BLR clouds may be more highly concentrated in the equatorial region of the AGNs and sparser at the poles (e.g., Elvis 2000). Regardless of their geometry, the emission line diagnostic tells us only about the BLR clouds irradiated by the continuum we observe and that we assume is coming from the jet.

All four of our objects are observed to have steep X-ray spectra. The early work of Guilbert et al. (1983) points out that a soft X-ray source heats circumnuclear gas to a single high-temperature phase $T \sim 10^6$ K, avoiding the creation of a stable two-phase medium and so inhibits the formation of large warm clouds in the BLR. Most AGN X-ray spectra are uniformly hard with spectral index $\alpha \sim -0.7$ compared to the much steeper spectra seen in these four (see Table 2) and most other HBLs.

Clearly the neutral gas column within the beam is low enough that no Lyman continuum decrement is seen. All four targets in this study have *FUSE* spectra covering the rest-frame Lyman limit and we see no significant change in continuum level on either side of this break. While it is not a strong constraint on the BLR neutral column, we can say $N_{\rm H\,I} \lesssim$ few $\times 10^{16}$ cm^{-2} for three of our four targets, on average within the beam. (The *FUSE* data for Mrk 501 are of poor quality and we can only set a limit $N_{\rm H\,I} \lesssim 1.5 \times 10^{17}$ cm^{-2} for this object.) This may be due to low optical depth, small covering fraction, or a combination of these effects, but in any case is consistent with a BL Lac BLR model which is optically thin.

In the optically thin regime, we can estimate the amount of warm gas in the BLR by assuming that there is one hydrogen atom for every Lyα photon emitted. The observed Lyα luminosities for these objects (Table 2) are so low that this assumption yields a BLR with only ∼10^{-4} to 10^{-5} $M_\odot$ of warm gas. Larger amounts of gas could be present if the few Lyα emitting clouds in the BLR are themselves optically thick at the Lyman limit so that most of the mass is not emitting any Lyα. This cloud geometry is however at variance with simple models of advection-dominated or Bondi–Hoyle accretion flows (ADAF; Narayan & Yi 1995; Allen et al. 2006). Assuming pressure equilibrium between the Lyα emitting clouds ($T \sim 10^{4.5}$ K) and a dominant coronal phase ($T \sim 10^6$ K) suggested by the Guilbert et al. scenario, and assuming a BLR size of a few parsecs, yields a mass of only ∼0.1 $M_\odot$. The amounts inferred to power the observed AGN (Cavaliere & D'Elia 2002, $\dot{m} \lesssim 10^{-2}$ $M_\odot$ yr^{-1}) are however much larger than the amounts that can be supplied by the BLR gas we infer to be present in these objects. There appears to be so little circumnuclear gas in BL Lacs that it is unclear how these sources power their relativistic jets.

It is worth considering the fact that these lines are not very broad at all, having FWHM $\lesssim$ 1000 km s^{-1}. (Sankrit et al. 1999 measure a weak, broad component to Lyα in M87 that could have FWHM $\lesssim$ 3000 km s^{-1}, although the continuum is poorly defined in their FOS spectrum.) By comparison, typical broad lines in Seyfert galaxies have FWHM many times higher, and the same is also true of the broad lines found in LBLs (Corbett et al. 2000; Scarpa & Falomo 1997; Vermeulen et al. 1995). In fact, the line widths we observe are much closer to

those seen in narrow, forbidden lines such as [O III]. Therefore, in addition to the possibilities presented above, the Lyα emitting material could be further out in these objects, at radii >10 pc, more typical of NLR gas. In this case there may be even less gas available for accretion power in the BLR.

4. CONCLUSIONS

We have measured weak, broad Lyα emission in three nearby HBLs and set a sensitive upper limit for a fourth one. Our Lyα luminosities are $\sim 10^{41}$ erg s^{-1} in three objects, an order of magnitude stronger than the weak, narrow optical emission lines that have been observed in a few HBLs ($\log L \leqslant 40$ erg s^{-1}; Rector et al. 2000; Sbarufatti et al. 2006). To the best of our knowledge this is the first detection of UV line emission from this rare class of AGN (although Lyα emission was observed in M87 by Sankrit et al. (1999)). BL Lacs are an important probe of physics at the very highest energies and our simultaneous measurements of both continuum and line emission will help constrain the models of their structure and kinematics.

From the observed data, we make a simple estimate of the number of ionizing photons produced by the jet and predict the Lyα line emission if this entire energy were radiated isotropically into optically thick BLR clouds. The predicted Lyα emission is 2–4 orders of magnitude larger than what is observed and we interpret this overprediction in two possible ways.

1. The overprediction is a symptom of relativistic beaming angle and broad line cloud covering fraction. For our two most extreme cases (Mrk 421 and PKS 2155−304), the beaming angles are somewhat smaller than predicted via other means and we needed to invoke a 1%–2% covering factor to be consistent with earlier beaming estimates for HBLs (Urry & Padovani 1995). However, it is equally plausible that the relativistic Γ for these two sources are much higher ($\sim$2–3$\times$) than the HBL population as a whole. But in the case of M87, for which Lyα and a weak UV continuum were detected using FOS (Sankrit et al. 1999), the overprediction factor of OPF $\geqslant 100$ is intriguing because little beaming is expected in our direction. In this case, a larger value of Γ does not explain the large OPF value since the large viewing angle (20°–25°; Heinz & Begelman 1997; Biretta et al. 1999) means that the continuum we observe is largely unbeamed. In this case, a small covering factor is the most likely cause of the weakness for the Lyα emission in M87.
2. Small covering factors inferred for M87 and possibly for Mrk 421 and PKS 2155−304 are quite similar to having optically thin and/or sparse clouds. So a quite plausible interpretation of the paucity of Lyα photons coming from these BL Lacs is that their BLRs are density-bounded, not ionization-bounded. This result was predicted for BL Lac objects by Guilbert et al. (1983) as a consequence of their steep X-ray continua.

Conclusion (2) can be extended in two ways. First, if the BLR clouds are optically thin, not all of the ionizing radiation is captured and converted to line emission and the Lyα luminosities are set by the total mass in warm gas in the BLR, 10^{-4} to 10^{-5} $M_{\odot}$. Assuming pressure balance in the BLR between these warm clouds and a hot medium as in the Guilbert et al. model requires that there is only $\sim$0.1 $M_{\odot}$ of gas in the BLR in toto. This is far too little to power the AGNs that we observe in these objects. Therefore, other fueling mechanisms need to be considered for BL Lac objects and their parent population, FR 1 radio galaxies. One obvious way around this conclusion is that, while there are very few BLR clouds around the nucleus in BL Lacs and FR 1 radio galaxies, these clouds are each very optically thick, so that a considerable amount of mass can be hidden by being shielded from the ionizing continuum. However, optically thick clouds seem at variance with an ADAF (Narayan & Yi 1995) scenario for fueling these sources.

Weak, broad Lyα line emission has been detected in the nucleus of the FR 1 radio galaxy M87 (Sankrit et al. 1999) with *HST*/FOS at comparable line luminosity to the Mrk 421 detection reported here. However, the low resolution (which blends the emission with damped Galactic Lyα absorption) and signal-to-noise (which poorly detects the UV continuum) is insufficient to determine the BLR parameters for M87 conclusively. There is also the issue that near-nuclear emission is thought to be due to shocks like in the spectra of LINERS (Dopita et al. 1997) so that the amount of photo-ionized Lyα could be even weaker than what is observed. Assuming the best available values for Γ and viewing angle in the case of M87 requires small covering factors in the ionization-bounded solution as in the cases of Mrk 421 and PKS 2155−304. Thus, as with the four BL Lacs, a density-bounded scenario should be considered for these low-luminosity AGNs which leave the question of their power source still open. The nucleus of M87 will be observed in *HST* Cycle 18 with COS obtaining much better resolution and signal-to-noise than the Sankrit et al. (1999) spectrum.

In addition to the above, one must now wonder about the differences between the LBL and HBL classes of BL Lacs. As already pointed out, a few LBLs have considerably more luminous broad-line emission than seen in these HBLs and other LBLs (e.g., Stickel et al. 1993; Scarpa & Falomo 1997; Rector & Stocke 2001; Corbett et al. 2000; Vermeulen et al. 1995), more consistent with the nebular hypothesis. In a purely viewing angle unification of LBLs and HBLs only a very tiny number of BLR clouds would be irradiated by a hard X-ray continuum (the LBL "region" of the celestial sphere as seen from the nucleus), while more BLR clouds would see the soft X-ray continuum characteristic of HBLs. In the few LBLs with luminous broad emission lines it appears likely that much larger amounts of gas are present in the BLR as quasi-stable broad-line clouds. If this is the case the off-axis ionizing continuum must be hard enough to permit BLR cloud formation, at variance with the simple viewing angle unification scheme outlined above. And also, given the much larger gas mass in the BLR, standard accretion can be a viable power source for these FR 2-like LBLs. These differences argue against a purely viewing angle based unification of all LBLs and HBLs.

Additional work is needed to flesh out the relationship between the two BL Lac classes, as well as the UV line-emission properties of BL Lacs in general. Mrk 421 and PKS 2005−489 were observed early in Cycle 17 as part of the COS Guaranteed Time Observation (GTO) program. Two higher-redshift BL Lacs (1ES 1028 + 511 and PMNJ 1103−2329) are scheduled for observation during Cycle 18 and we will analyze their Lyα emission properties. Two additional BL Lacs at unknown redshift (S5 0716 + 714 and 1ES 1553 + 113) will also be observed and we will look closely for emission features by which their systemic redshifts can be determined. The latter object was observed briefly in 2009 and the redshift was constrained via intervening Lyα absorbers ($z > 0.4$; Danforth et al. 2010). A re-observation of M87 with *HST*/COS and STIS

can be used to determine if the Lyα emission in FR 1s is consistent with expectations of unified schemes. Detection of both Lyα and C IV emission can test whether the gas is ionized by shocks or by a UV continuum. The spatial resolution along the STIS slit will determine how much of the observed Lyα and continuum flux is truly nuclear.

It is our pleasure to acknowledge the many thousands of people who made the *HST* Servicing Mission 4 the huge success that it was. We furthermore thank Steve Penton, Stéphane Beland, and the other members of the COS ERO and GTO teams for their work on initial data calibration and verification and Lisa Winter for the Mrk 817 fit parameters. J.T.S. acknowledges a College Scholar Fellowship from the College of Arts & Sciences, University of Colorado at Boulder for support during this research work. J.T.S. also acknowledges the Center for Computational Cosmology, Durham University, the Institute of Astronomy, Cambridge University, and the Specola Vaticana, Castel Gandolfo for hospitality during portions of this work. C.W.D. acknowledges a fruitful discussion with members of the KIPAC consortium. This work was supported by NASA grants NNX08AC146 and NAS5-98043 to the University of Colorado at Boulder.

Facilities: HST(COS), HST(STIS), HST(GHRS)

REFERENCES

Abdo, A., et al. 2009, ApJS, 183, 46
Acciari, V. A., et al. 2009, ApJ, 703, 169
Allen, S. W., Dunn, R. J. H., Fabian, A. C., Taylor, G. B., & Reynolds, C. S. 2006, MNRAS, 372, 21
Antonucci, R. R. J. 1984, ApJ, 278, 499
Biretta, J. A., Sparks, W. B., & Macchetto, F. 1999, ApJ, 520, 612
Brinkmann, W., Papadakis, I. E., den Herder, J. W. A., & Haberl, F. 2003, A&A, 402, 929
Brinkmann, W., Papadakis, I. E., Raeth, C., Mimica, P., & Haberl, F. 2005, A&A, 443, 397
Brinkmann, W., Siebert, J., Kollgaard, R. I., & Thomas, H.-C. 1996, A&A, 313, 356
Brinkmann, W., et al. 2001, A&A, 365, L162
Browne, I. W. A., & Marchã, M. J. M. 1993, MNRAS, 261, 795
Cavaliere, A., & D'Elia, V. 2002, ApJ, 571, 226
Collinge, M. J., et al. 2005, AJ, 129, 2542
Corbett, E. A., Robinson, A., Axon, D. J., & Hough, J. H. 2000, MNRAS, 311, 485
Danforth, C. W., Keeney, B. A., Stocke, J. T., Shull, J. M., & Yao, Y. 2010, ApJ, 720, 976
Donato, D., Sambruna, R. M., & Gliozzi, M. 2005, A&A, 433, 1163
Dopita, M. A., Koratkur, A. P., Allen, M. G., Tsvetanov, Z. I., Ford, H. C., Bicknell, G. V., & Sutherland, R. S. 1997, ApJ, 490, 202
Edelson, R., Griffiths, G., Markowitz, A., Sembay, S., Turner, M. J. L., & Warwick, R. 2001, ApJ, 554, 274
Elvis, M. 2000, ApJ, 545, 63
Fanaroff, B. L., & Riley, J. M. 1974, MNRAS, 167, 31
Fitzpatrick, E. L. 1999, PASP, 111, 63
Foschini, L., et al. 2006, A&A, 453, 829
Fossati, G., Maraschi, L., Celotti, A., Comastri, A., & Ghisellini, G. 1998, MNRAS, 299, 433
Georganopoulos, M., & Marscher, A. P. 1998, ApJ, 506, 621
Ghisellini, G., Celotti, A., & Costamante, L. 2002, A&A, 386, 833
Ghisellini, G., Celotti, A., Fossati, G., Maraschi, L., & Comastri, A. 1998, MNRAS, 301, 451
Ghisellini, G., & Tavecchio, F. 2008, MNRAS, 387, 1669
Ghisellini, G., Tavecchio, F., Foschini, L., Ghirlanda, G., Maraschi, L., & Celotti, A. 2010, MNRAS, 402, 497
Giroletti, M., Giovannini, G., Cotton, W. D., Taylor, G. B., Pérez-Torres, M. A., Chiaberge, M., & Edwards, P. G. 2008, A&A, 488, 905
Giroletti, M., Giovannini, G., Taylor, G. B., & Falomo, R. 2006, ApJ, 646, 801
Guetta, D., Ghisellini, G., Lazzati, D., & Celotti, A. 2004, A&A, 421, 877
Guilbert, P. W., McCray, R., & Fabian, A. C. 1983, ApJ, 266, 466
Haardt, F., & Madau, P. 1996, ApJ, 461, 20
Heinz, S., & Begelman, M. C. 1997, ApJ, 490, 653
Hovatta, T., Valtaoja, E., Tornikoski, M., & Lähteenmäki, A. 2009, A&A, 494, 527
Hutchings, J. B., & Neff, S. G. 1992, AJ, 104, 1
Indebetouw, R., & Shull, J. M. 2004, ApJ, 607, 309
Jannuzi, B. T., Smith, P. S., & Elston, R. 1994, ApJ, 480, 130
Maraschi, L., Foschini, L., Ghisellini, G., Tavecchio, F., & Sambruna, R. M. 2008, MNRAS, 391, 1981
Massaro, F., Tramacere, A., Cavaliere, A., Perri, M., & Giommi, P. 2008, A&A, 478, 395
Narayan, R., & Yi, I. 1995, ApJ, 452, 710
Nieppola, E., Valtaoja, E., Tornikoski, M., Hovatta, T., & Kotiranta, M. 2008, A&A, 488, 867
Osterbrock, D. E., & Ferland, G. J. 2006, in Astrophysics of Gaseous Nebulae and Active Galactic Nuclei, ed. D. E. Osterbrock & G. J. Ferland (2nd ed.; Sausalito, CA: Univ. Science Books)
Osterman, S., et al. 2010, Ap&SS, submitted (arXiv:1012.5827)
Padovani, P., Costamante, L., Giommi, P., Ghisellini, G., Celotti, A., & Wolter, A. 2004, MNRAS, 347, 1282
Padovani, P., & Giommi, P. 1995, ApJ, 444, 567
Padovani, P., et al. 2001, MNRAS, 328, 931
Penton, S. V., Stocke, J. T., & Shull, J. M. 2000, ApJS, 130, 121
Perlman, E. S., & Stocke, J. T. 1993, ApJ, 406, 430
Perlman, E. S., Stocke, J. T., Wang, Q. D., & Morris, S. L. 1996, ApJ, 456, 451
Perlman, E. S., et al. 2005, ApJ, 625, 727
Ravasio, M., Tagliaferri, G., Ghisellini, G., & Tavecchio, F. 2004, A&A, 424, 841
Rector, T. A., & Stocke, J. T. 2001, AJ, 122, 565
Rector, T. A., Stocke, J. T., Perlman, E. S., Morris, S. L., & Gioia, I. M. 2000, AJ, 120, 1626
Sankrit, R., Sembach, K. R., & Canizares, C. R. 1999, ApJ, 527, 733
Sbarufatti, B., Treves, A., & Falomo, R. 2005, ApJ, 635, 173
Sbarufatti, B., Treves, A., Falomo, R., Heidt, J., Kotilainen, J., & Scarpa, R. 2000, AJ, 132, 1
Scarpa, R., & Falomo, R. 1997, A&A, 325, 109
Scarpa, R., Urry, C. M., Falomo, R., Pesce, J. E., & Treves, A. 2000, ApJ, 532, 740
Sembay, S., Edelson, R., Markowitz, A., Griffiths, R. G., & Turner, M. J. L. 2002, ApJ, 574, 634
Shull, J. M., & van Steenberg, M. E. 1985, ApJ, 294, 599
Stickel, M., Fried, J. W., & Kühr, H. 1993, A&AS, 98, 393
Tramacere, A., Massaro, F., & Cavaliere, A. 2007a, A&A, 466, 521
Tramacere, A., et al. 2007b, A&A, 467, 501
Urry, C. M., & Padovani, P. 1995, PASP, 107, 803
Urry, C. M., Sambruna, R. M., Worrall, D. M., Kollgaard, R. I., Feigelson, E. D., Perlman, E. S., & Stocke, J. T. 1996, ApJ, 463, 424
Vermeulen, R. C., Ogle, P. M., Tran, H. D., Browne, I. W. A., Cohen, M. H., Readhead, A. C. S., Taylor, G. B., & Goodrich, R. W. 1995, ApJ, 452, L5
Winter, L. M., et al. 2011, ApJ, 728, 28
Wurtz, R., Stocke, J. T., & Yee, H. K. C. 1996, ApJS, 103, 109
Zhang, Y. H. 2008, ApJ, 682, 789
Zhang, Y. H., Bai, J. M., Zhang, S. N., Treves, A., Maraschi, L., & Celotti, A. 2006a, ApJ, 651, 782
Zhang, Y. H., Treves, A., Maraschi, L., Bai, J. M., & Liu, F. K. 2006b, ApJ, 637, 699